Acta Phys. Hung. B 20/1 (2004) 000–000

QUANTUM
ELECTRONICS

Optical Implementation of Two Programmable Quantum Measurement Devices

A. Černoch[1], J. Soubusta[1,2], J. Fiurášek[1] and M. Dušek[1]

[1] Department of Optics, Palacký University,
17. listopadu 50, 772 00 Olomouc, Czech Republic

[2] Joint Laboratory of Optics of Palacký University and Institute of Physics of Academy of Sciences of the Czech Republic,
17. listopadu 50A, 772 00 Olomouc, Czech Republic

Received 1 January 2004

Abstract. We present an optical realization of an adjustable discriminator of non-orthogonal quantum states and a programmable phase-covariant quantum multimeter. Both devices utilize polarization states of photon pairs generated by spontaneous parametric down-conversion. The experimental realization is based on the fact that two Bell states can be distinguished solely by means of linear optics. The first device discriminates unambiguously between two non-orthogonal polarization states of the data qubit. The selection of the states that should be discriminated is controlled by the quantum state of the program qubit. The second device can perform any von Neumann measurement on a single qubit represented by a polarization state from the equator of the Bloch sphere. Also in this case the measurement basis is selected by the state of the program qubit.

Keywords: programmable discriminator, quantum multimeter
PACS: 03.67.Mn, 42.50.Dv

1. Introduction

In this article we deal with the most essential part of all quantum apparatus, namely quantum measurement [1–4]. Recently the universal quantum measurement devices - quantum multimeters - were introduced [5–9]. Their main advantage is the possibility to program the apparatus by the quantum states of another qubit system called program register. These states can be in principle unknown and mutually nonorthogonal.

The paper is organised as follows: the programmable quantum state discrim-

1589-9535/04/ $ 20.00

inator is discussed in Sec. 2 and phase-covariant quantum multimeter in Sec. 3. Both devices are set by the polarization state of the program qubit and then they distinguish between two states of the data qubit. Whole measurement devices are composed of linear optics only, a balanced beam-splitter, polarizing beam-splitters and photodetectors. Two Bell states can be distinguished and the other two Bell states correspond to inconclusive results.

2. Programmable quantum-state discriminator

2.1. Theory

A general *unknown* quantum state cannot be determined completely by a measurement performed on a single copy of the system. The situation is different if *a priori* knowledge is available [1–3] – e.g., if one works only with states from a certain discrete set. Even quantum states that are mutually non-orthogonal can be distinguished with a certain probability provided they are linearly independent (for a review see Ref. [10]). There are, in fact, two different optimal discrimination strategies [11]: First, to determine the state with the minimum probability of errors [1,2]. Second, unambiguous or error-free discrimination. In this case the measurement result is always correct, but there is a nonzero probability of an inconclusive result [12–16]. The first experiment, designed for the discrimination of two linearly polarized states of light, was done by Huttner *et al.* [17]. The interest in the quantum state discrimination is not only "academic" – unambiguous state discrimination can be used, e.g., as an efficient attack in quantum cryptography [18].

In this paper we focus our attention to the unambiguous state discrimination. Let us suppose that we want to discriminate unambiguously between two non-orthogonal states. However, we would like to be able to work with different pairs of states. The programming of the discriminator to work with given states is controlled by preparing a program register in the corresponding state [5].

Let us have two (non-orthogonal) input states of a qubit that should be discriminated:

$$|\phi_d^{\pm}\rangle = a|H_d\rangle \pm b|V_d\rangle, \tag{1}$$

where $|H\rangle$ and $|V\rangle$ denote horizontal and vertical polarization. The complex numbers a and b are determined by orientation ϑ and ellipticity $\tan\varepsilon$ of the polarization ellipse (see Fig. 1):

$$a = \cos\varepsilon\cos\vartheta + \mathrm{i}\sin\varepsilon\sin\vartheta,\ b = \cos\varepsilon\sin\vartheta - \mathrm{i}\sin\varepsilon\sin\vartheta. \tag{2}$$

Subscript "d" stays for "data". Note that these states are supposed to be symmetrically located around the state $|H_{\mathrm{d}}\rangle$. In addition let us have a program qubit in a state (index "p" denotes "program") $|\phi_p\rangle = a|H_p\rangle + b|V_p\rangle$. Then the total state of the data and program qubit acquires a form

$$|\phi_d^{\pm}\rangle \otimes |\phi_p\rangle = \sqrt{2}\left[\frac{a^2 \pm b^2}{2}|\Phi^+\rangle + \frac{a^2 \mp b^2}{2}|\Phi^-\rangle + ab|\Psi^{\pm}\rangle\right], \tag{3}$$

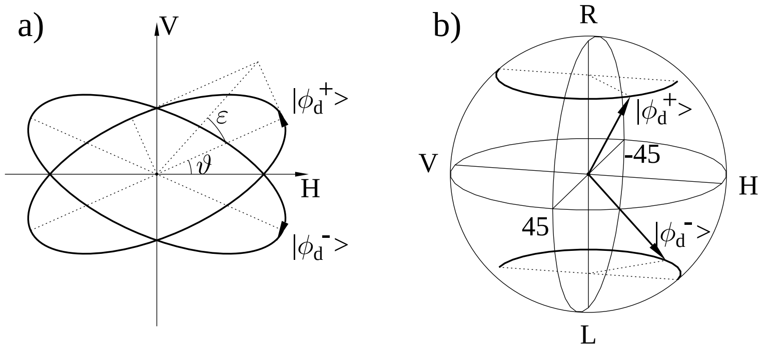

Fig. 1. Example of the measured data states $|\phi_d^+\rangle$ and $|\phi_d^-\rangle$ ($\varepsilon = 24°$, $\vartheta = 24°$) : a) polarization ellipses, b) Stokes vectors.

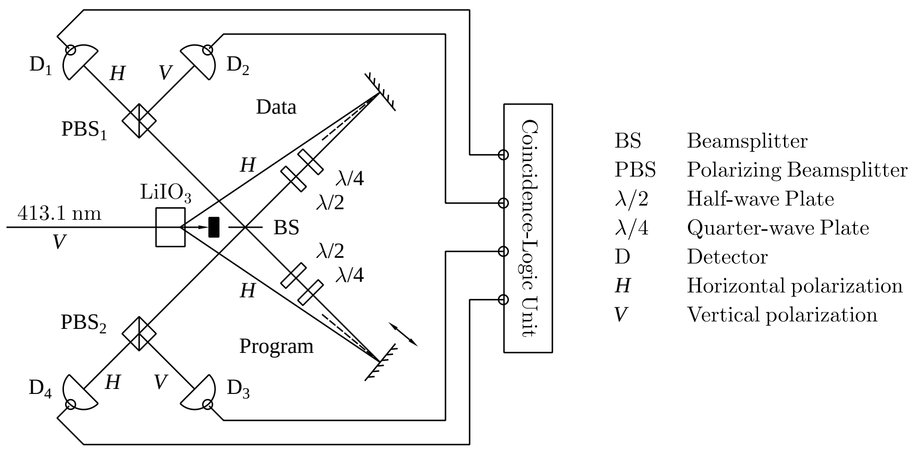

Fig. 2. Scheme of the measurement setup.

where $|\Psi^\pm\rangle$ and $|\Phi^\pm\rangle$ are the Bell states

$$|\Psi^\pm\rangle = \frac{1}{\sqrt{2}}\left(|H_d\rangle|V_p\rangle \pm |V_d\rangle|H_p\rangle\right), \quad |\Phi^\pm\rangle = \frac{1}{\sqrt{2}}\left(|H_d\rangle|H_p\rangle \pm |V_d\rangle|V_p\rangle\right). \qquad (4)$$

If we are able to distinguish between the two Bell states $|\Psi^+\rangle$ and $|\Psi^-\rangle$ then we can unambiguously discriminated states $|\phi_d^+\rangle$ and $|\phi_d^-\rangle$.

The probability of successful discrimination is $p = 2|ab|^2 = 2(|a|^2 - |a|^4)$.

2.2. Experiment

Pairs of entangled photons are generated in the process of spontaneous parametric down-conversion in $LiIO_3$ nonlinear crystal pumped by cw Kr-ion laser at 413.1 nm. Generated photons are horizontally polarized and centered at 826.2 nm. Required polarization states are prepared by means of rotating wave plates: $\lambda/4$ is rotated by angle $\alpha = \pm\varepsilon$; $\lambda/2$ is rotated by angle $\beta = \pm(\varepsilon + \vartheta)/2$. Both photons overlap at a nonpolarizing beam splitter (BS) forming Hong-Ou-Mandel interferometer (HOM) [19], the lengths of both arms are equalized by scanning a mirror in one arm. The output beams from the BS pass polarization beam splitters (PBS) to distinguish horizontal and vertical components. Then the beams are filtered by cut-off filters and circular apertures and coupled into multimode fibers. D_1, …, D_4 denote Perkin-Elmer single-photon counting modules (quantum efficiencies $\approx 50\%$, dark counts about 150/s). The signals from detectors are processed by our home made 4-input-coincidence unit and the results are transfered to a PC.

2.3. Measurement result

First we scanned the HOM interference dip for diagonal linear polarizations. The measured rate of coincidences between D_1 and D_4 or D_2 and D_3 is plotted in Fig. 3a) as a function of the mirror position. Then the coincidences corresponding to Bell states $|\Psi^+\rangle$ and $|\Psi^-\rangle$ were scanned in the same range in order to gain the value of C_{sh} away from the interference dip for the normalization purposes. In the zero position, if detectors D_1 and D_2 or D_3 and D_4 click together, the Bell state $|\Psi^+\rangle$ is detected, so $|\phi_d^+\rangle$ is recognized. Whereas, if detectors D_1 and D_3 or D_2 or D_4 click together, the Bell state $|\Psi^-\rangle$ is detected, so the state $|\phi_d^-\rangle$ is recognized. The other two Bell states lead to an inconclusive result, because no coincidence count occur.

In the following text we use this simplified notation: C^{++} denotes the detection rate of $|\Psi^+\rangle$ when the input state was $|\phi_d^+\rangle \otimes |\phi_p\rangle$; C^{-+} mean detection rate of $|\Psi^-\rangle$ for input state $|\phi_d^+\rangle \otimes |\phi_p\rangle$; etc. Figure 3b) shows scans of coincidence rates C^{++}, C^{+-}, C^{-+} and C^{--} as a function of the mirror position. Main measurements plotted in Fig. 4 show the dependence of the coincidence rates as a function of angle ϑ: a) for linear polarization ($\varepsilon = 0°$); and b) for elliptical polarization ($\varepsilon = 24°$). Figure. 5 illustrates the probability of successful discrimination calculated from the experimental data measured for four different ellipticities as follows

$$P_{succ} = \frac{1}{2}\left[\frac{C^{++}}{2(C_{sh}^{++} + C_{sh}^{-+})} + \frac{C^{--}}{2(C_{sh}^{--} + C_{sh}^{+-})}\right]. \tag{5}$$

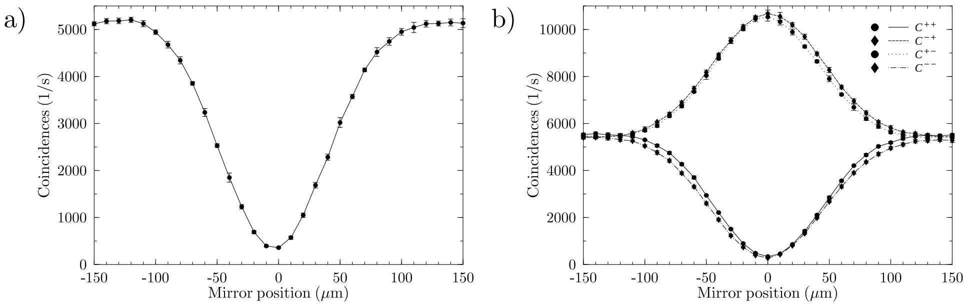

Fig. 3. a) Hong-Ou-Mandel interference dip measured for linear polarization, $\vartheta = 45°$. b) Coincidences measured for input states $|\phi_d^+\rangle$ and $|\phi_d^-\rangle$ with parameters $\varepsilon = 0$, $\vartheta = 45°$, as a function of mirror displacement.

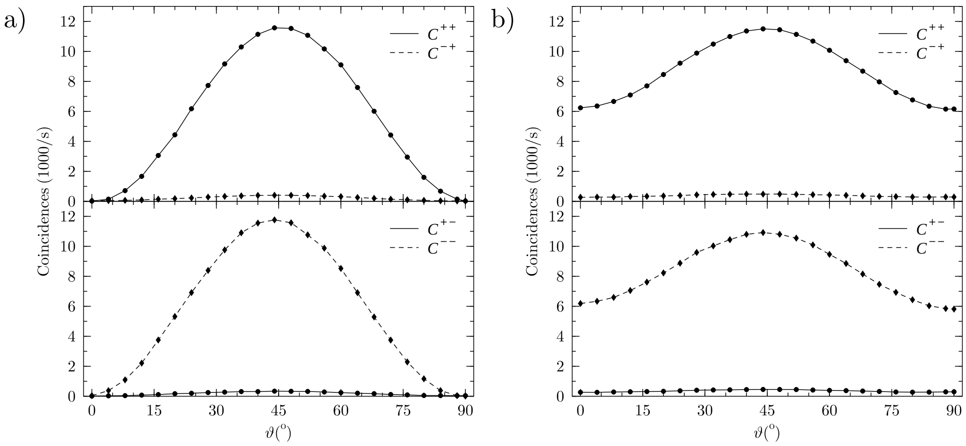

Fig. 4. Coincidences measured for a) linear input polarizations ($\varepsilon = 0°$) and b) elliptical input polarization. ($\varepsilon = 24°$)

3. Phase-covariant quantum multimeter

In this section, our aim is to perform von Neumann measurements on a single qubit in any basis $\{|\psi_+\rangle, |\psi_-\rangle\}$ located on the equator of the Bloch sphere

$$|\psi_\pm(\phi)\rangle = \frac{1}{\sqrt{2}}\left(|0\rangle \pm e^{\mathrm{i}\phi}|1\rangle\right), \quad \phi \in [0, 2\pi). \tag{6}$$

The particular measurement basis is selected by a quantum state of a program register. It is impossible to perfectly encode such projective measurement into states in finite-dimensional Hilbert space [4, 5], but it is possible to encode POVMs that

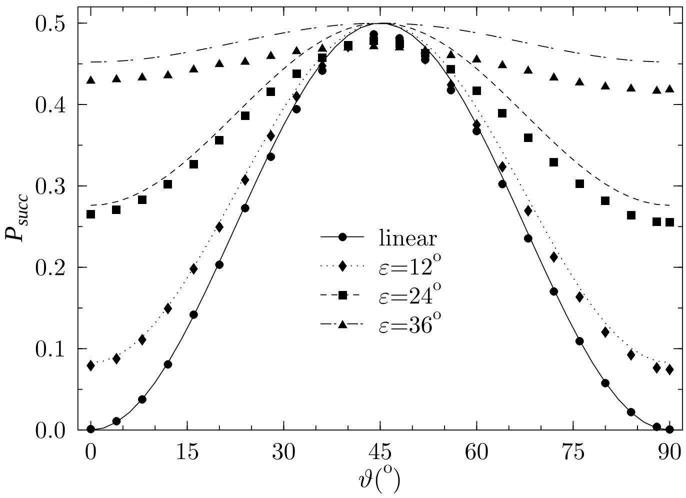

Fig. 5. Probability of success for all measured ellipticities. (Points are measured data, lines correspond to theoretical predictions.)

represent, in certain sense, the best approximation of required projective measurements.

As in the previous section there are two methods: deterministic multimeter and probabilistic one. The optimal probabilistic multimeter should minimize the error rate of the *conclusive* outcomes for the fixed fraction of *inconclusive* results. As a limit case it is possible to get an error-free operation.

3.1. Theory

The optimal (fixed) POVM acting on data and program qubits together for one-qubit program reads [8, 9]:

$$\begin{aligned} \Pi_{\pm} &= |\Psi^{\pm}\rangle\langle\Psi^{\pm}| + \frac{1-\eta}{2}\left(|\Phi^{+}\rangle\langle\Phi^{+}| + |\Phi^{-}\rangle\langle\Phi^{-}|\right), \\ \Pi_{?} &= \eta\left(|\Phi^{+}\rangle\langle\Phi^{+}| + |\Phi^{-}\rangle\langle\Phi^{-}|\right). \end{aligned} \tag{7}$$

The factor η parametrize a smooth transition from a deterministic error-prone multimeter ($\eta = 0$) to a probabilistic error-free one ($\eta = 1$). Again, $|\Psi^{\pm}\rangle$ and $|\Phi^{\pm}\rangle$ are the Bell states. Probability of an inconclusive result for this multimeter is $P_I = \eta/2$, and the formula for the average fidelity reads $F = (3 - 2P_I)/(4(1 - P_I))$. Thus for ambiguous multimeter we have $F = 3/4$ and $P_I = 0$, whilst for error-free operation we obtain $F = 1$ and $P_I = 1/2$.

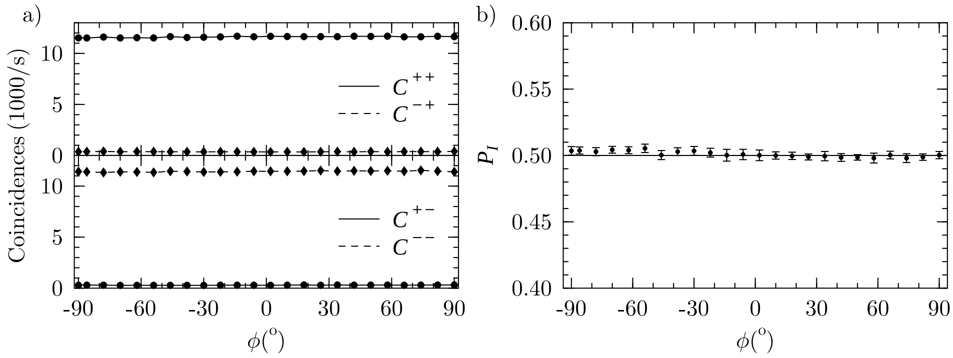

Fig. 6. a) Coincidence rates; and b) Probability of Inconclusive result for unambiguous operation as a function of phase ϕ. Solid line represents theoretical value $P_I = 1/2$.

3.2. Experimental realization

This experiment can also be implemented using the setup shown in Fig 2. Two *logical values* of qubit $|0\rangle$ and $|1\rangle$ are represented by linear horizontal $|H\rangle$ and vertical $|V\rangle$ polarization states. Desired states $|\psi_{\pm}(\phi)\rangle$ are prepared by means of rotating wave plates: $\lambda/4$ is rotated by angle $\alpha = \mp\phi/2$ and $\lambda/2$ is rotated by $\beta = \pm(90^o - \phi)/4$ with respect to horizontal plane. As in the previous section, detection of $|\Psi^+\rangle$ corresponds to the recognition of the basis state $|\psi_+(\phi)\rangle$; detection of $|\Psi^-\rangle$ corresponds to basis state $|\psi_-(\phi)\rangle$. Everything else means an inconclusive result.

Inconclusive-result rate is a *complement* of conclusive-result rate. In our measurement, the relative error rate (with respect to all conclusive results) - i.e., a fraction of events when we get $|\Psi^+\rangle$ instead of $|\Psi^-\rangle$ or vice versa, is about 3%. It is mainly due to unbalance of the splitting ratio of the BS and non-ideal overlap of spatial modes.

Probability of inconclusive result P_I can be obtained as

$$P_I = 1 - \frac{1}{2}\left[\frac{C^{++} + C^{-+}}{2(C_{sh}^{++} + C_{sh}^{-+})} + \frac{C^{--} + C^{+-}}{2(C_{sh}^{--} + C_{sh}^{+-})}\right]. \tag{8}$$

Measured probability of inconclusive result P_I (Fig. 6b) is in good agreement with theoretical value 1/2 and, as expected, it does not depend on the measurement basis represented by the phase ϕ.

4. Conclusions

Measurement on the data qubit can be quite efficiently controled by the quantum state of the program register. Classical setting of the angle between the states that shall be unambiguously discriminated and a classical description of a measurement basis in case of projective phase-covariant measurement would require infinitely many bits of classical information, while only one quantum bit suffices in the present case to obtain an *error-free* (although probabilistic) operation.

Acknowledgments

This research was supported under the project LN00A015 of the Ministry of Education of the Czech Republic. J.F. also acknowledges support from the EU under the project CHIC (IST-2001-33578). M.D. acknowledges support from the EU project SECOQC (IST-2002-506813).

References

1. C.W. Helstrom, *Quantum Detection and Estimation Theory* (Academic Press, New York, 1976).
2. A.S. Holevo, *Probabilistic and Quantum Aspects of Quantum Theory* (North-Holland, Amsterdam, 1982).
3. A. Peres, *Quantum Theory: Concepts and Methods*(Kluwer, Dordrecht, 1993).
4. M.A. Nielsen and I.L. Chuang, *Quantum Computation and Quantum Information* (Cambridge Univ. Press, Cambridge, 2000).
5. M. Dušek and V. Bužek, *Phys. Rev. A* **66**, (2002) 022112.
6. J. Fiurášek, M. Dušek and R. Filip, *Phys. Rev. Lett.* **89**, (2002) 190401; *Fortschritte der Physik* **51**, (2003) 107.
7. M. Hendrych, M Dušek, R Filip, and J Fiurášek, *Physics Letters A* **310**, (2003) 95.
8. J. Fiurášek and M. Dušek, *Phys. Rev. A* **69**, (2004) 032302; e-print: quant-ph/0308111.
9. J. Soubusta, A. Černoch, J. Fiurášek, M. Dušek, *Phys. Rev. A* **69**, (2004) 052321.
10. A. Chefles, *Contemp. Phys.* **41**, (2001) 401.
11. S.M. Barnett, *Fortschritte der Physik* **49**, (2001) 909.
12. I.D. Ivanovic, *Phys. Lett. A* **123**, (1987) 257.
13. D. Dieks, *Phys. Lett. A* **126**, (1988) 303.
14. A. Peres, *Phys. Lett. A* **128**, (1988) 19.
15. G. Jaeger and A. Shimony, *Phys. Lett. A* **197**, (1995) 83.
16. A. Chefles and S.M. Barnett, *Phys. Lett. A* **250**, (1998) 223.
17. B. Huttner, A. Muller, J.D. Gautier, H. Zbinden, and N. Gisin, *Phys. Rev. A***54**, (1996) 3783.
18. M. Dušek, M. Jahma, N. Lütkenhaus, *Phys. Rev. A***62**, (2000) 022306.
19. C.K. Hong, Z.Y. Ou, and L. Mandel, *Phys. Rev. Lett.***59**, (1987) 2044.